

An Integrated Fault Isolation and Prognosis Method for Electric Drive Systems of Battery Electric Vehicles

N.Sakthiselvam¹, S.Srinivasan², S.Raajkumar³, M.Selvakumari⁴, S.Saravanan⁵

*UG Scholar^{1,2,3}, Associate Professor⁴, Professor⁵
Department of Electrical and Electronics Engineering
Muthayammal Engineering College – Tamilnadu*

Abstract— The electric drive system is a key subsystem of battery electric vehicles (BEVs). Abnormalities in the electric drive system components may lead to performance degradation in the drive system and, more severely, loss of power in the vehicle. This article presents an integrated prognosis system for early detection and isolation of the electric drive system and component faults. The system first calculates multiple health features, known as health indicators derived from the available onboard sensor signals. Then, an integrated prognostic and fault isolation strategy is used to isolate the root cause of electric drive faults by monitoring the performance of the multiple health indicators. The prognostic system uses a hierarchical approach: it first determines if there is a degradation in the electric drive system by comparing the system achieved torque with the estimated torque and, then, goes further to check multiple component-level health indicators for the various components comprising an electric drive system, including motor stator winding, three-phase current sensors, and resolver. After a component has been detected to degrade to a certain level, the prognosis system sends out an alert before the severe performance reduction of the drive system occurs, thus protecting the customers from loss of propulsion and walk home situations.

I. INTRODUCTION

Electrical drive technology converts electrical energy from the power supply system or from a battery into mechanical energy and transmits the resulting force into motion. Many applications that make our daily lives easier – like lifts, escalators, gate drives, washing machines, mixers, electric razors, etc. The Vehicle Technologies Office (VTO) supports research and development (R&D) to reduce the cost and improve the performance of innovative electric drive devices, components, and systems. For a general overview of electric drive vehicles, see the Alternative Fuels Data Center's pages on Hybrid and Plug in Electric Vehicles. Electric vehicles (EVs) have been around since the late 1800s.

II. EXISTING SYSTEM

In existing model short circuit fault analysis happen is existing model algorithm is the important problem in existing structure Nowadays, the use of electric vehicles (EVs) has expanded due to various environmental and economic benefits. However, given that EVs are considered as loads that are not fixed in one place and can be connected to different parts of the power system at different times, challenges are undeniable. With the growing pollution problems, greenhouse effects and increasing prices of the petroleum products, the transport sector has covered its way to the use of Electric Vehicles (EVs). Large scale use of EVs requires an increase in number and complexities of Electric Vehicle Charging Stations within distribution network. An understanding of charging station configuration and its fault behaviors is important in order to develop a comprehensive protection system. Charging time reduction is one of the key goals in making electric vehicles user-friendly. In this context, fast DC charging offers an interesting opportunity. It allows for reducing charging times to ranges of 10 to 20 minutes. The SAE J1772 standard defines three levels of fast DC charging as DC Level 1 200/450 V, up to 36 kW (80 A); DC Level 2 - 200/450 V, up to 90 kW (200 A) and DC Level 3 200/600 V DC (proposed) up to 240 kW (400 A). All levels use off-board electric vehicle supply equipment (EVSE). modelling and simulation of an electric vehicle charging station for fast DC charging are proposed and formulated in an educational way in order to allow its implementation and further research on the topic. In the following sections, important aspects of an EV charging station model are developed. In Section II, the Proposed methodology of the circuit is considered. Control methods for DC charging of EVs and the charging station and fault analysis of the system.

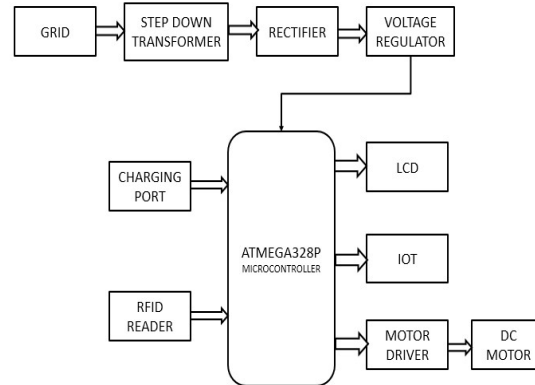


Fig.1. Block Diagram

III. PROPOSED SYSTEM

The health indicator calculation module calculates multiple health indicators HI_1, HI_2, \dots, HI_k based on the signals of interest. These health indicators represent the health features of the various components and can be used to detect various failure modes. The health indicators are then fed into the prognostic algorithm that applies a rule-based fault isolation strategy that combines the outputs from the multiple health indicators to make a prognostic decision as to which component is degrading and is affecting the performance of the electric drive system, i.e., the root cause of the performance degradation. This article uses a hierarchical approach: the algorithm first detects if there is performance degradation in the overall electric drive system by looking at the system-level health indicator and then goes deeper to the lower level (component level) health indicators to isolate the faulty component. The multiple health indicators are presented in Section IV. In real applications, the health indicators can be calculated online based on the available measurements or control signals, but the prognostic decision is not made until we see consistent results after several drive cycles. This is to avoid any false alarms or instantaneous fault that can be misleading, which usually happens in reality due to unexpected driving conditions.

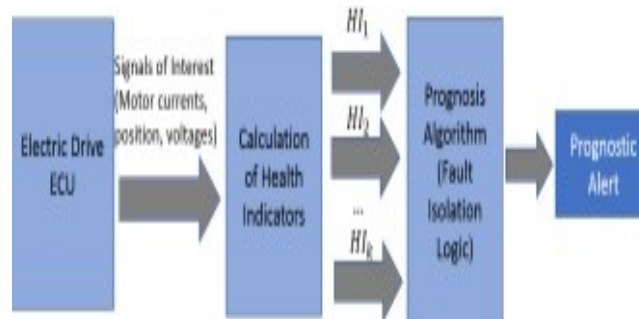


Fig.2. Block Diagram of Internal Fault

In real applications, based on the data from driving cycle tests on a vehicle dyno and from real-world road tests, this condition can always be found for at least 1–2 s per trip when the vehicle is slowing down from higher speed, while the electric motor torque decreases from positive to zero. The winding health indicator is described by Fig. 5, where u_{dref} represents the actual reference d-axis voltage, u^*_{dref} stands for the reference in the healthy case, and i_{qref} and i_{dref} represent the reference q- and d-axis currents, respectively. In real applications, u_{dref} is usually obtained by the current regulator and is available from the electric motor controller. In this health indicator, it is straightforward that the effect of resistance fault on the health indicator is $HI_2 = r_{sidref}$.

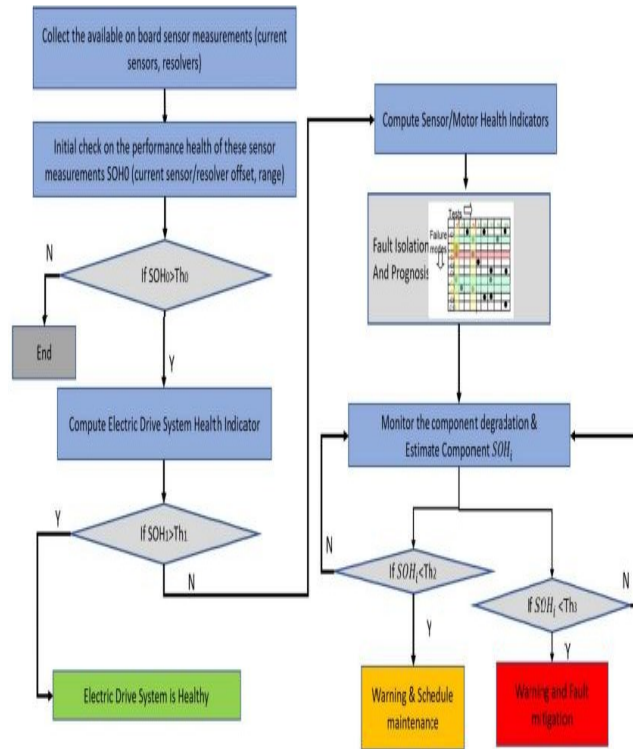
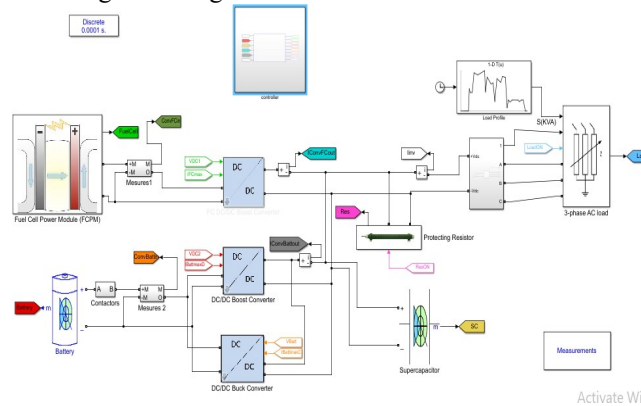


Fig.3. Algorithm of Electrical Drive System

Description of the Hierarchical Prognostic Algorithm After we collect the onboard sensor signals, we perform an



initial check on the sensor range/performance. If there are any out-of-range faults in the current sensors/resolver, the diagnostics would be triggered, and the rest of the process would not proceed. On the other hand, if the performance of the sensors is within the predefined threshold (Th0), then the prognostic system will first perform the electric drive health check by checking the performance of the electric drive system-level health indicator.

IV. SIMULATION

The ampere-hour-based method consists of measuring the input and output current at battery terminals and using this information, to compute the SOC. This method is easy to implement; however, it is susceptible to errors due to imprecise measurements, which forces the utilization of high-cost sensors. The OCV method assumes that there is a relationship between the measurements. Future profiles for the battery discharge current are computed after a characterization of the usage profile for each experimental test. The failure condition is defined as the moment in which the demand of electrical power exceed optimization problem. Particularly during the experimental tests reported in this work, this failure event is related to a situation in which the constraint for the minimum voltage in the terminals of the battery (cut-off voltage, V_c) is violated. The latter means that if the predicted voltage at the battery pack reaches V_c , at that time is considered that the fault occurs. It is worth remembering that the V_c , is given by the battery manufacturer, and for the batteries used in this work, it is equal to

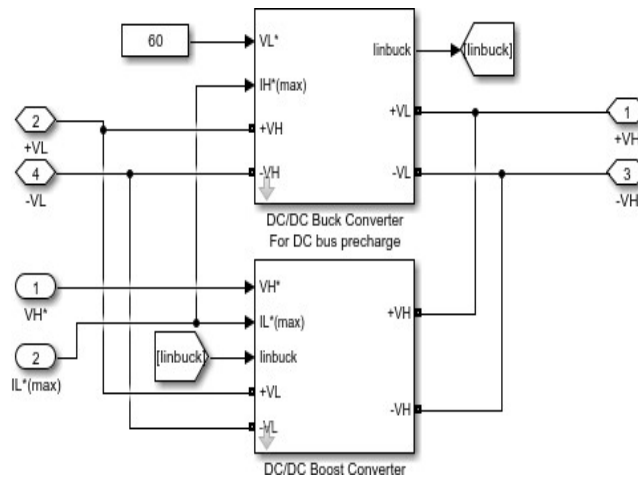


Fig.4. Simulation Diagram

33V. The ampere-hour-based method consists of measuring the input and output current at battery terminals and using this information, to compute the SOC. This method is easy to implement; however, it is susceptible to errors due to imprecise measurements, which forces the utilization of high-cost sensors. The cut-off value of 33 V. Indeed, if the FT-PDF is computed solely based on information about the predicted voltage, then it cannot be used to provide a reasonable expectation

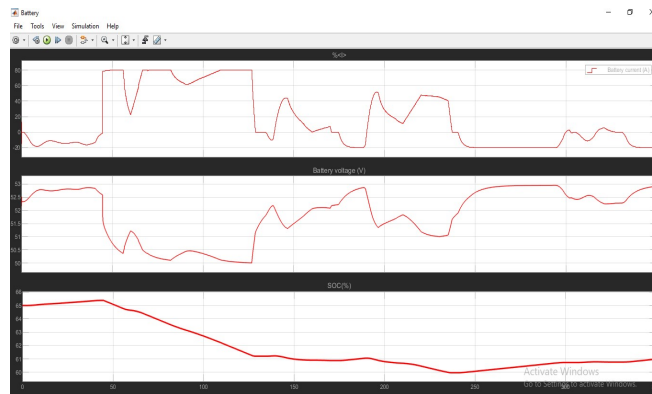


Fig.5. DC to DC Converter

Since the Markov chain Characterization of the future operating profile is not able to anticipate a sudden change in the power consumption that takes place at $t = 5866[s]$. Interestingly enough, the representation of the conditions that define a possible fault in the system: as soon as the measured power intersects the predicted SoMPA 95% confidence interval the failure event takes place, thus validating the proposed approach as a method to define the maximum power requirements that the system may handle without interruptions in the system operational continuity.

Fig.6. Battery Current and Voltage SOC

Battery is inferior to the maximum power available. Fig. 4 shows estimates for the magnitude of the battery internal impedance, SOC, and SoMPA in the Data Set #2. It noteworthy that this data set corresponds to a situation where the bicycle is driven through a route with elevation. Similarly to the results obtained for Data Set #1, estimates of the internal impedance range between $0.2[\Omega]$ to $0.3[\Omega]$ while the battery SOC varies between Internal Impedance, SOC, and SOMPA estimates - Data Set #3. 0.9 and 0.6, meaning that at the beginning of the test.

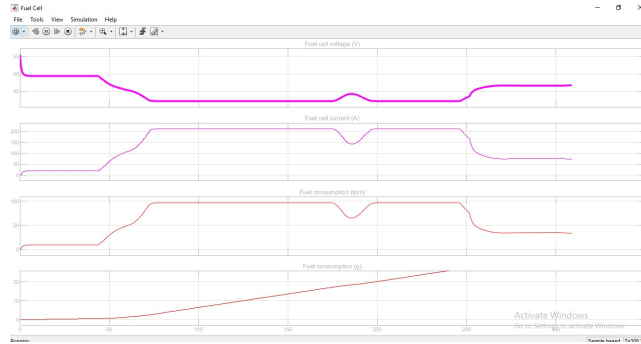


Fig.7. Input and Output waveform

It should be noted that in this experiment, the BMS of the battery bank activates the under-voltage protection when the SOC is approximately 0.6. The latter is caused by the fact that the power required by the bicycle to follow the route is very high, forcing a significant voltage drop and activating the low-voltage protection of the system [2]. This situation implies that the power required from the battery during this test route reached the estimated SoMPA, as shown in the last graph

V. HARDWARE CIRCUIT

The ac voltage, typically 220V rms, is connected to a transformer, which steps that ac voltage down to the level of the desired dc output. This section focuses on the results obtained with the proposed SoMPA estimator. Notice that for all validation sets, the initial SoC is arbitrarily initialized at 50% of the true value to analyse the impact of erroneous initial condition. The results for each validation set are as follows. shows (i) the expectation of the SoMPA and the confidence interval (of 95%) of the SoMPA estimate at each time instant, and (ii) the PDF of SoMPA of the estimator at some arbitrary time instants for validation sets #1, #2 and #3, respectively [3]. The proposed SoMPA estimator computes the expected value as well as the confidence interval for a given confidence level. The proposed framework allows us to compute the conditional SoMPA PDF estimate at any arbitrary time instant. Fig. 6 and e depicts the performance of the PF-based PDF estimate at moments in which the filter has converged (uncertainty associated with the estimate is mainly due to measurement X or Y is 500 volts. Since only one diode can conduct at any instant, the maximum voltage that can be rectified at any instant is 500 volts. The maximum voltage that appears across the load resistor is nearly-but never exceeds-500 v0lts, as result of the small voltage drop across the diode. In the bridge rectifier shown in view B, the maximum voltage that can be rectified is the full secondary voltage, which is 1000 volts. Therefore, the peak output voltage across the load resistor is nearly 1000 volts. With both circuits using the same transformer, the bridge rectifier circuit produces a higher output voltage than the conventional full-wave rectifier circuit. In a method to predict the maximum power is proposed, using multi-limited methods and the Extended Kalman Filter (EKF). Multi-limited methods combine features from the voltage-limited, current-limited and SOC-limited methods to improve precision and robustness in the predictionstage.

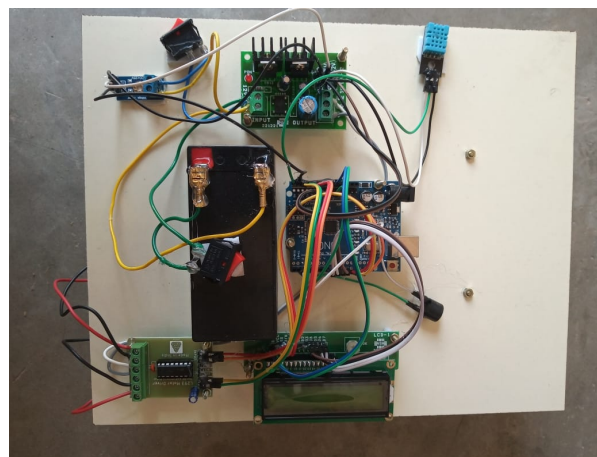


Fig.8. Hardware Circuit

Particularly, during the experimental tests reported in this work, this failure event is related to a situation in which

the constraint for the minimum voltage in the terminals of the battery (cut-off voltage) is violated. It should be highlighted that this research effort does not include a long term analysis of the battery State of Health (SOH), since the main objective is to prognosticate failures that may occur after a few hours of operation at the most.

VII.CONCLUSION

Integrated fault isolation and prognosis system for the key components in an electric drive. The prognosis system takes the measurements from the three-phase current sensors, resolver, and the control inputs of reference voltages. It first detects if there is performance degradation in the drive system by comparing the estimated torque based on the dc input power and power losses, with the calculated achieved torque based on motor currents. If a performance degradation has been found, then it proceeds to isolate the root cause of the error, which either is due to a motor fault caused by the stator winding degradation, or a sensor fault due to resolver fault, or one of the three-phase current sensor faults. The method to isolate the fault is to compare the performance of various component-level health indicators in parallel. The performance of the health indicators and the prognosis algorithm is validated both on a motor dyno and a vehicle dyno, where a production drive motor is used. The results show that the prognosis system is successful in detecting and isolating the component fault and is also capable of predicting the drive system performance degradation; thus, it can protect customers from loss of propulsion and walk home situations.

REFERENCES

- [1] P. Krause, O. Wasynczuk, and S. D. Pekarek, *Electromechanical Motion Devices*, vol. 90. Hoboken, NJ, USA: Wiley, 2012.
- [2] E.-S. Jun, S.-Y. Park, and S. Kwak, "A comprehensive double-vector approach to alleviate common-mode voltage in three-phase voltage source inverters with a predictive control algorithm," *Electronics*, vol. 8, no. 8, p. 872, Aug. 2019.
- [3] R. R. Schoen, T. G. Habetler, F. Kamran, and R. G. Bartfield, "Motor bearing damage detection using stator current monitoring," *IEEE Trans. Ind. Appl.*, vol. 31, no. 6, pp. 1274–1279, Nov. 1995.
- [4] B. Li, M.-Y. Chow, Y. Tipsuwan, and J. C. Hung, "Neural-network based motor rolling bearing fault diagnosis," *IEEE Trans. Ind. Electron.*, vol. 47, no. 5, pp. 1060–1069, Oct. 2000.
- [5] J. R. Stack, T. G. Habetler, and R. G. Harley, "Fault classification and fault signature production for rolling element bearings in electric machines," *IEEE Trans. Ind. Appl.*, vol. 40, no. 3, pp. 735–739, May 2004.
- [6] J. A. Rosero, J. Cusido, A. Garcia, J. A. Ortega, and L. Romeral, "Broken bearings and eccentricity fault detection for a permanent magnet synchronous motor," in *Proc. 32nd Annu. Conf. IEEE Ind. Electron. (IECON)*, Nov. 2006, pp. 964–969.
- [7] F. Meinguet, P. Sandulescu, X. Kestelyn, and E. Semail, "A method for fault detection and isolation based on the processing of multiple diagnostic indices: Application to inverter faults in AC drives," *IEEE Trans. Veh. Technol.*, vol. 62, no. 3, pp. 995–1009, Mar. 2013.
- [8] K. Rothenhagen and F. W. Fuchs, "Performance of diagnosis methods for IGBT open circuit faults in three phase voltage source inverters for AC variable speed drives," in *Proc. Eur. Conf. Power Electron. Appl.*, 2005, p. 10.
- [9] B. Cai, Y. Zhao, H. Liu, and M. Xie, "A data-driven fault diagnosis methodology in three-phase inverters for PMSM drive systems," *IEEE Trans. Power Electron.*, vol. 32, no. 7, pp. 5590–5600, Jul. 2017.
- [10] Y. Lu Murphey, M. A. Masrur, Z. Chen, and B. Zhang, "Model-based fault diagnosis in electric drives using machine learning," *IEEE/ASME Trans. Mechatronics*, vol. 11, no. 3, pp. 290–303, Jun. 2006.
- [11] F. Schemmel, K. Bauer, and M. Kaufhold, "Reliability and statistical lifetime-prognosis of motor winding insulation in low-voltage power drive systems," *IEEE Elect. Insul. Mag.*, vol. 25, no. 4, pp. 6–13, Jul. 2009.
- [12] S. M. A. Cruz and A. J. M. Cardoso, "Stator winding fault diagnosis in three-phase synchronous and asynchronous motors, by the extended Park's vector approach," *IEEE Trans. Ind. Appl.*, vol. 37, no. 5, pp. 1227–1233, Sep. 2001.
- [13] S. Nandi, H. A. Toliyat, and X. Li, "Condition monitoring and fault diagnosis of electrical motors—A review," *IEEE Trans. Energy Convers.*, vol. 20, no. 4, pp. 719–729, Dec. 2005.
- [14] M. A. S. K. Khan and M. A. Rahman, "Development and implementation of a novel fault diagnostic and protection technique for IPM motor drives," *IEEE Trans. Ind. Electron.*, vol. 56, no. 1, pp. 85–92, Jan. 2009.
- [15] M. A. Mazzeletti, G. R. Bossio, C. H. De Angelo, and D. R. EspinozaTrejo, "A model-based strategy for interturn short-circuit fault diagnosis in PMSM," *IEEE Trans. Ind. Electron.*, vol. 64, no. 9, pp. 7218–7228, Sep. 2017.